Drug Design, Development and Therapy

Dovepress
open access to scientific and medical research

Open Access Full Text Article

ORIGINAL RESEARCH

Identification of novel multitargeted PPARα/γ/δ pan agonists by core hopping of rosiglitazone

This article was published in the following Dove Press journal:
Drug Design, Development and Therapy
7 November 2014
Number of times this article has been viewed

Xue-Jiao Wang[1]
Jun Zhang[1]
Shu-Qing Wang[1]
Wei-Ren Xu[2]
Xian-Chao Cheng[1]
Run-Ling Wang[1]

[1]Tianjin Key Laboratory on Technologies Enabling Development of Clinical Therapeutics and Diagnostics (Theranostics), School of Pharmacy, Tianjin Medical University, Tianjin, People's Republic of China; [2]Tianjin Key Laboratory of Molecular Design and Drug Discovery, Tianjin Institute of Pharmaceutical Research, Tianjin, People's Republic of China

Abstract: The thiazolidinedione class peroxisome proliferator-activated receptor gamma (PPARγ) agonists are restricted in clinical use as antidiabetic agents because of side effects such as edema, weight gain, and heart failure. The single and selective agonism of PPARγ is the main cause of these side effects. Multitargeted PPARα/γ/δ pan agonist development is the hot topic in the antidiabetic drug research field. In order to identify PPARα/γ/δ pan agonists, a compound database was established by core hopping of rosiglitazone, which was then docked into a PPARα/γ/δ active site to screen out a number of candidate compounds with a higher docking score and better interaction with the active site. Further, absorption, distribution, metabolism, excretion, and toxicity prediction was done to give eight compounds. Molecular dynamics simulation of the representative Cpd#1 showed more favorable binding conformation for PPARs receptor than the original ligand. Cpd#1 could act as a PPARα/γ/δ pan agonist for novel antidiabetic drug research.

Keywords: PPARs, diabetes, docking, molecular dynamics simulation, ADMET

Introduction

Peroxisome proliferator-activated receptors (PPARs) are nuclear ligand-activated transcription factors and include three subtypes, namely PPARα, PPARγ, and PPARδ.[1–3] The drugs targeting PPARs mainly include: 1) PPARγ agonists[4] such as rosiglitazone and pioglitazone, which are used as antidiabetic drugs and also possess anti-inflammatory or antineoplastic activities,[5,6] and 2) PPARα agonists such as fenofibrate and bezafibrate, which are used as antilipemic drugs (Figure 1).[7,8] Rosiglitazone and pioglitazone have shown side effects in clinical use, such as liver function abnormity, edema, and weight gain.[9] Especially in 2007, Nissen and Wolski[10] reported the cardiac safety of rosiglitazone, which showed that singly selective agonism of PPARγ not only enhanced insulin sensitivity and the therapeutic effect of insulin metabolism but also caused edema, weight gain, and the potential risk of heart failure.

In recent years, some novel PPARs concepts appeared in the antidiabetic drug research area, such as multitargeted cooperative PPARα/γ dual agonists and PPARα/γ/δ pan agonists. These multitargeted agonists could cooperatively improve glucose and lipid metabolism. They could not only effectively control blood sugar but also reduce the content of triglyceride, free fatty acid, and low-density lipoprotein, as well as increase high-density lipoprotein concentration, thus having a preventive effect on cardiovascular complications of type 2 diabetes patients. Some of these multitargeted PPARs agonists have entered clinical trials and represent promising PPARs drug research.[11–13]

The pharmacophore of PPARs agonists consists of the polar head, linker, and hydrophobic tail. The polar head of PPARs agonists could form a hydrogen bond with Tyr residue at the AF-2 region, producing a transactivation effect. The hydrophobic

Correspondence: Xian-Chao Cheng; Run-Ling Wang
School of Pharmacy, Tianjin Medical University, No. 22 Qixiangtai Road, Tianjin 300070, People's Republic of China
Tel +86 22 8333 6658
Email chengxianchao@aliyun.com; wangrunling@tijmu.edu.cn

submit your manuscript | www.dovepress.com
Dovepress
http://dx.doi.org/10.2147/DDDT.S70383

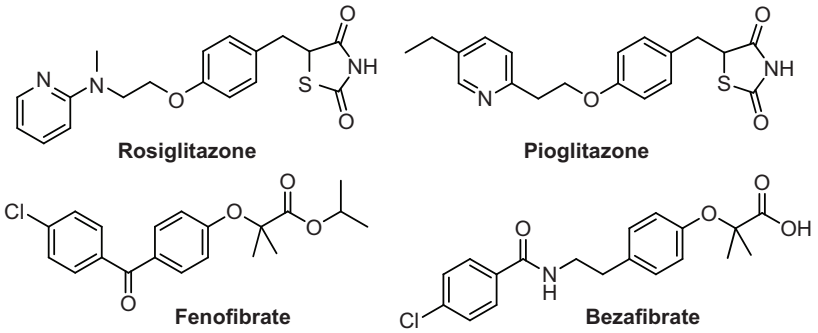

Figure 1 Thiazolidinediones and fibrates.

tail of PPARs agonists could bind to the residues at the active site entrance, affecting subtype selectivity. This indicates that by modification of the polar head and hydrophobic tail, various pharmacological effects can be produced, such as PPARα/γ dual agonistic activity and PPARα/γ/δ pan agonistic activity.

In our previous research, using GW409544 as the starting point, by means of "core hopping" and "glide docking" techniques, a novel class of PPARα/γ dual agonists was discovered.[14] In this paper, starting from rosiglitazone as the lead compound, using a core hopping approach, the polar head, linker, and hydrophobic tail of rosiglitazone were modified to produce various compounds. These compounds were then screened by docking and absorption, distribution, metabolism, excretion, and toxicity (ADMET) prediction to discover some excellent PPARα/γ/δ pan agonists. Molecular dynamics simulations of the representative Cpd#1 with PPARα/γ/δ were also done to study the binding details (Figure 2).

Materials and methods

Preparation of PPAR receptors structures

The crystal structures of PPARα, PPARγ, and PPARδ receptors were downloaded from the Protein Data Bank (PDB) with PDB identification numbers 1I7G, 2PRG, and 2ZNP, respectively.[15–17] The preparation of these receptors was performed on the Protein Preparation Wizard embedded in Schrodinger 2009. The process of preparing receptors included assigning bond orders, adding hydrogen, treating metals, treating disulfides, deleting waters, alleviating potential steric clashes, adjusting formal charges, minimizing proteins with the OPLS (Optimized Potentials for Liquid Simulation) 2005 force field,[18] and refining the protein by limiting value of root mean square deviation (RMSD) to 0.50 Å as the constraint. Then, the original ligand was centered and redocked into the binding site to generate a docking box for molecular docking.

Core hopping and docking

The Core Hopping module in Schrodinger 2009 software was used to modify the polar head, linker, and hydrophobic tail of rosiglitazone (Figure 2).[19] Core hopping is a docking algorithm that has the functions of fragment-based replacing and molecular docking.[20–22] The first step of core hopping was to define the points at which the cores were attached to the scaffold. It was performed in the Define Combinations Step from the Combinatorial Screening panel. The second step was to define "the receptor grid file", which was done in the Receptor Preparation panel. The third step was to prepare the cores attached to the scaffold using fragment database derived from ZINC.[23,24] The fourth step was to align and dock the entire molecular structure built up by the core and scaffold. The cores were sorted and filtered by goodness of alignment and then redocked into the receptor after attaching the scaffold, followed by using the docking scores to sort the final molecules.[25–27] The original ligand AZ242, rosiglitazone, and TIPP204 were used as positive control compounds.

ADMET prediction

The ADMET module of Discovery Studio 3.1 was used to predict pharmacokinetics and toxicity of the compounds (Figure 2). Taking rosiglitazone as control, the compounds as a mol2 file were imported into the ADMET Descriptors module and the Toxicity Prediction Extensible and Toxicity Prediction TOPKAT modules, respectively, obtaining pharmacokinetics and toxicity parameters.

Molecular dynamics simulation

In order to study the binding stability of compounds with PPARs active site, the 10ns molecular dynamics simulations were performed using the open GROMACS 4.0 package for Linux (Figure 2).[28] Before the simulations, the coordinate file and topology file were prepared[29] and the water box was constructed and filled with simple point charge water solution,

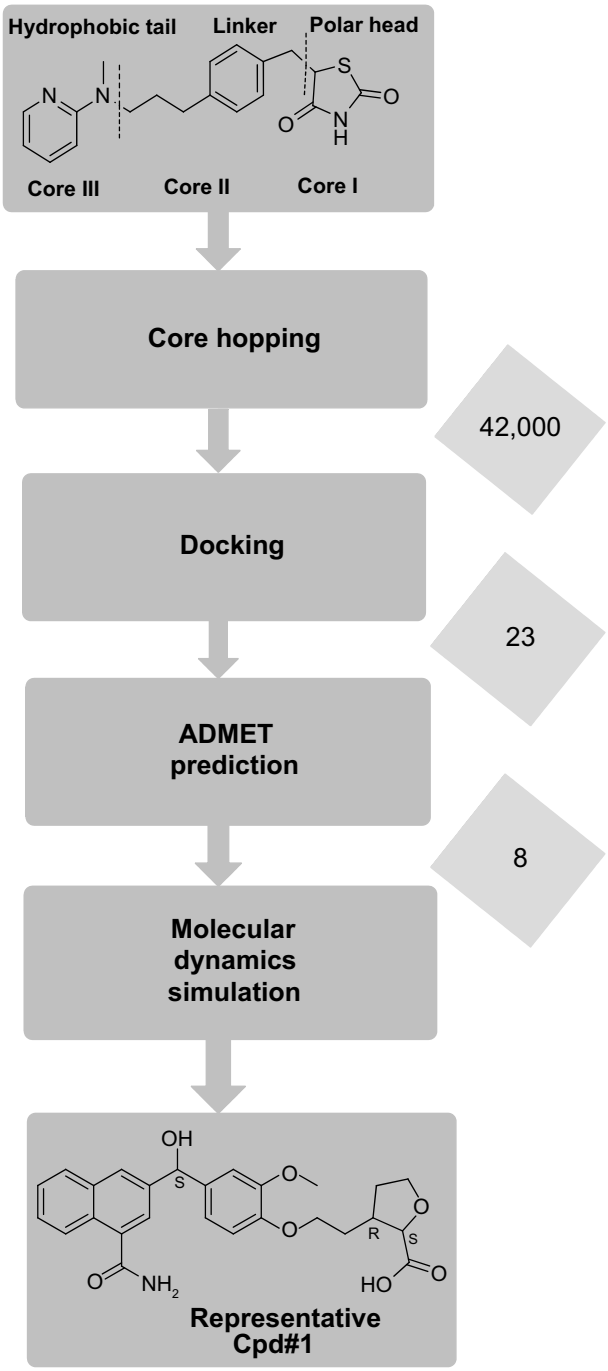

Figure 2 Discovery of multitargeted peroxisome proliferator-activated receptor agonists by core hopping of rosiglitazone.
Abbreviation: ADMET, absorption, distribution, metabolism, excretion, and toxicity.

which was then neutralized by sodium ions or chloride ions.[30,31] The 1,000-step energy minimization of the system was performed using the steepest descending method. The NVT (constant number, volume and temperature) ensembles were used with temperature being maintained at 300 K. The cutoff radius of van der Waals interaction was 1.4 nm, and particle mesh Ewald algorithm was used for the electrostatic interaction.[32,33] The Linear Constraint Solver algorithm was used for all of the bond restriction.[34–36]

Results and discussion

Ligand binding domains of the PPAR receptors

The X-ray crystallography studies showed that the ligand binding domain of the PPARs was composed of 12α-helix and 4 antiparalleled β-sheet. The three subtypes of PPARs were 60%–70% sequence similarities with RMSD between Cα atoms <1 Å. In addition, the ligand binding domain of the PPARα/γ/δ formed a Y-shaped hydrophobic pocket with a volume of about 1,300 Å^3. The AF-2 region of H12 helix played an important role in the process of the activation of PPARs. As for PPARδ, the AF-2 region was significantly narrower, which was not suitable for binding ligands with a larger polar head.[37]

Core hopping and docking

A total of 42,000 compounds were obtained by core hopping of rosiglitazone. These compounds were docked into PPARα (pdb 1I7G), PPARγ (pdb 2PRG), and PPARδ (pdb 2ZNP), respectively, screening out 23 compounds with higher docking scores and better binding poses than the original ligands. Further ADMET prediction studies produced the top eight compounds (Table 1). The docking scores of these compounds with PPARα and PPARγ were higher than the original ligand AZ242 and rosiglitazone, respectively. The docking scores of these compounds with PPARδ were somewhat lower than the original ligand TIPP204. In addition, the hydrogen bond distances between compounds and PPARs were <3.20 Å,[38,39] and the values were equal to the original ligand.

The docking mode of the representative Cpd#1 with the active site of PPARα/γ/δ receptors is shown in Figure 3. The carboxyl acidic head of Cpd#1 formed hydrogen bonds with the key residues of PPARα (Ser280, Tyr314, Tyr464, and His440), PPARγ (Ser289, His323, Tyr473, and His449), and PPARδ (His323, His449, and Tyr473) receptors, respectively. The aromatic hydrophobic tail and the linker of Cpd#1 bound to PPARα/γ/δ with similar conformations to the original ligand AZ242, rosiglitazone, and TIPP204, respectively.

ADMET prediction

The development of the PPARα/γ dual agonist muraglitazar has been discontinued during clinical trials because of danger and mortality rate of cardiovascular

Table 1 The docking results of rosiglitazone analogues with peroxisome proliferator-activated receptor (PPAR)α/γ/δ receptors

Entry	Structure	Docking score – lg (Kd)			Hydrogen bond distance (Å)		
		PPARα	PPARγ	PPARδ	PPARα	PPARγ	PPARδ
Cpd#1	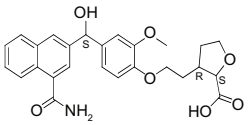	12.51	12.61	13.19	Ser280:1.919 Tyr314:1.881 His440:2.029 Tyr464:1.648	Ser289:1.533 His323:2.384 His449:2.808 Tyr473:2.877	Thr289:1.808 His323:1.865 His449:1.963 Tyr473:1.559
Cpd#2	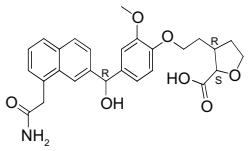	12.38	12.39	13.34	Ser280:2.101 Tyr314:1.934 His440:1.949 Tyr464:1.742	Ser289:1.583 His323:2.389 His449:1.981 Tyr473:2.694	Thr289:1.970 His323:1.935 His449:1.653 Tyr473:1.735
Cpd#3	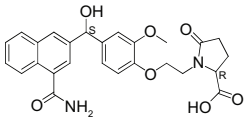	13.08	12.26	12.49	Ser280:1.796 Tyr314:2.010 His440:2.042 Tyr464:1.758	Ser289:1.581 His323:2.253 His449:2.925 Tyr473:2.684	Thr289:1.912 His323:1.882 His449:1.693 Tyr473:1.769
Cpd#4	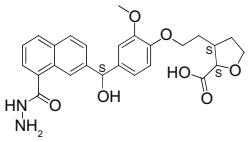	12.67	12.15	13.15	Ser280:2.085 Tyr314:1.951 His440:2.101 Tyr464:1.580	Ser289:2.405 His323:3.011 His449:1.753 Tyr473:2.823	Thr289:1.849 His323:1.896 His449:1.891 Tyr473:1.590
Cpd#5	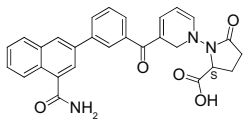	11.61	12.16	14.39	Ser280:2.053 Tyr314:2.154 His440:2.711 Tyr464:1.943	Ser289:1.574 His323:2.212 His449:3.071 Tyr473:2.667	Thr289:1.903 His323:1.707 His449:1.817 Tyr473:1.637
Cpd#6	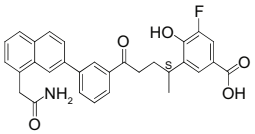	11.97	11.44	12.42	Ser280:1.665 Tyr314:1.948 His440:2.344 Tyr464:2.019	Ser289:1.663 His323:2.253 His449:2.915 Tyr473:2.662	Thr289:1.895 His323:2.031 His449:2.019 Tyr473:1.537
Cpd#7	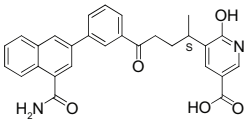	11.40	11.11	11.87	Ser280:1.638 Tyr314:2.133 His440:1.866 Tyr464:2.026	Ser289:2.186 His323:2.742 His449:2.186 Tyr473:2.610	Thr289:1.910 His323:2.041 His449:1.996 Tyr473:1.545
Cpd#8	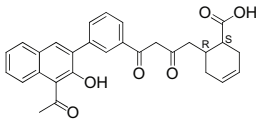	11.61	10.62	11.57	Ser280:1.917 Tyr314:2.498 His440:2.158 Tyr464:1.815	Ser289:2.751 His323:2.745 His449:2.659 Tyr473:2.052	Thr289:1.994 His323:2.974 His449:1.717 Tyr473:2.146
AZ242	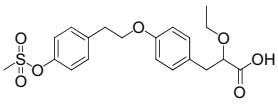	10.63			Ser280:1.640 Tyr314:1.958 His440:1.884 Tyr464:2.040		
Rosiglitazone	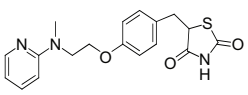		10.38			Ser289:1.943 His323:2.021 His449:2.202 Tyr473:2.484	
TIPP204	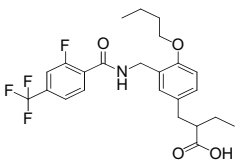			15.59			Thr289:1.836 His323:1.780 His449:1.929 Tyr473:1.588

Notes: The original ligands AZ242, rosiglitazone, and TIPP204 were used as positive control. Hydrogen bond distance (N-H···O and so on) is acceptable under 3.20 Å.

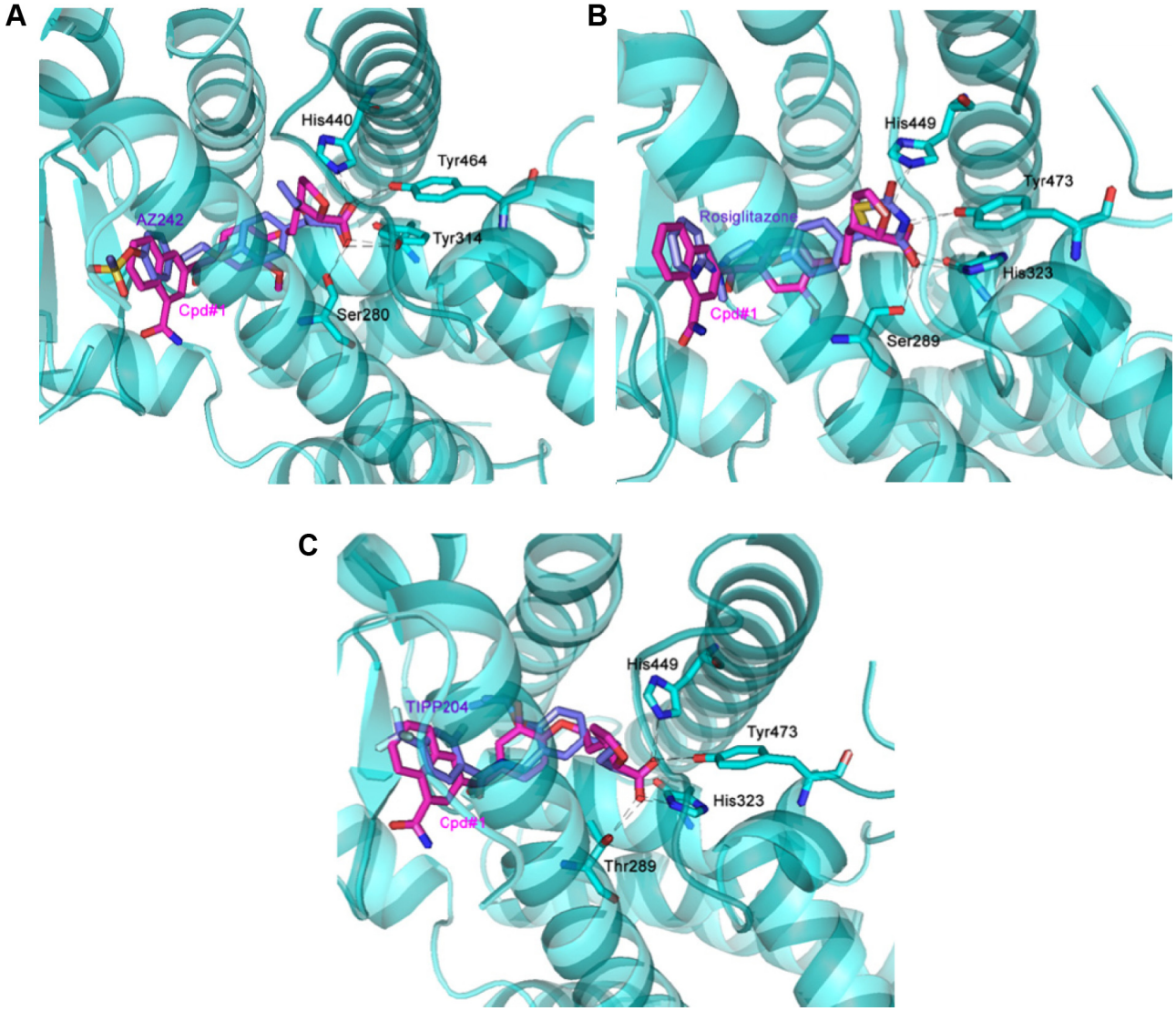

Figure 3 The docking mode of representative Cpd#1 with the active site of peroxisome proliferator-activated receptor (PPAR)α (**A**), PPARγ (**B**), and PPARδ (**C**).
Note: The original ligands AZ242 (left), rosiglitazone (middle), and TIPP204 (right) are colored in purple.

Table 2 The ADMET prediction results of rosiglitazone analogues

Entry	MW (g/mol)	$AlogP_{98}$	PSA-2D	QplogS	nON	nOHNH	SL3 computed probability of mutagenicity (%)
Cpd#1	464.487	1.277	131.13	−5.058	7	2	0
Cpd#2	478.514	1.312	131.14	−3.537	7	2	0
Cpd#3	477.486	0.512	142.21	−4.106	7	2	0
Cpd#4	478.494	0.889	145.24	−4.397	8	2	0
Cpd#5	480.491	0.706	123.84	−5.810	6	1	0
Cpd#6	499.530	5.490	117.69	−6.132	5	3	0
Cpd#7	468.501	4.638	130.57	−6.249	6	3	0
Cpd#8	470.513	4.517	108.74	−6.469	6	2	0
AZ242	408.465	3.367	107.51	−4.295	7	1	0
Rosiglitazone	357.427	3.268	96.83	−4.289	6	1	0.001
TIPP204	469.469	6.121	75.63	−6.919	4	2	0

Abbreviations: ADMET, absorption, distribution, metabolism, excretion, and toxicity; MW, molecular weight; $AlogP_{98}$, atom-based LogP (octanol/water); PSA-2D, 2D fast polar surface area; QplogS, predicted aqueous solubility; nON, number of hydrogen bond acceptors; nOHNH, number of hydrogen bond donors.

events.[40] Thus, the prediction of drug ADME/Tox was crucial and could reduce the risk of the drug development. The pharmacokinetics and toxicity of the top eight compounds were predicted using the ADMET module of Discovery Studio 3.1. The molecular weight (MW), octanol–water partition coefficient ($AlogP_{98}$), polar surface area (PSA-2D), aqueous solubility (QplogS), number of hydrogen bond acceptors (nON), number of hydrogen bond donors (nOHNH), and mutagenicity of rosiglitazone analogues are listed in Table 2, respectively. These compounds accorded with Lipinski's rule of five (Mol_MW<500, $0.4<AlogP_{98}<5.6$, nOHNH<5, nON<10, 7<PSA-2D<200, 0.5<QplogS<6.5),[41,42] and the values were equal to the positive control AZ242, rosiglitazone, and TIPP204. The probabilities of mutagenicity of these compounds were also lower than for rosiglitazone.

Molecular dynamics trajectory analysis

In order to study the dynamics behaviors and the binding stability of the PPARs–Cpd#1 complex, the 10ns molecular dynamics simulations were performed on PPARs–apo, PPARs–original ligand complex, and PPARs–Cpd#1 complex.

The RMSD versus the simulation time was considered as a significant criterion to evaluate the stability of dynamic behavior. The final RMSD values for all the simulation systems were <0.8 nm (Figure 4). After 3ns, the RMSD values for Cpd#1–PPARs system (red) was the lowest one among these three simulation trajectories.

In order to study the dynamic details of key residues interacted with the ligand, the root mean square fluctuations (RMSF) of all the side chain residues were obtained. The RMSF curve of PPARs–Cpd#1 complex was similar to that of PPARs–original ligand complex (Figure 4). At the key residues of PPARα such as Ser280 (the pink area), Tyr314 (the conch area), Tyr464 (the cyan area), and His440 (the coral area), the RMSF values of the PPARα–Cpd#1 complex were somewhat lower than those of the PPARα–original ligand complex and PPARα–apo form. As for PPARγ/δ, similar circumstances existed just as with PPARα. These molecular dynamics simulation trajectories indicated that PPARs became more stable after binding Cpd#1.

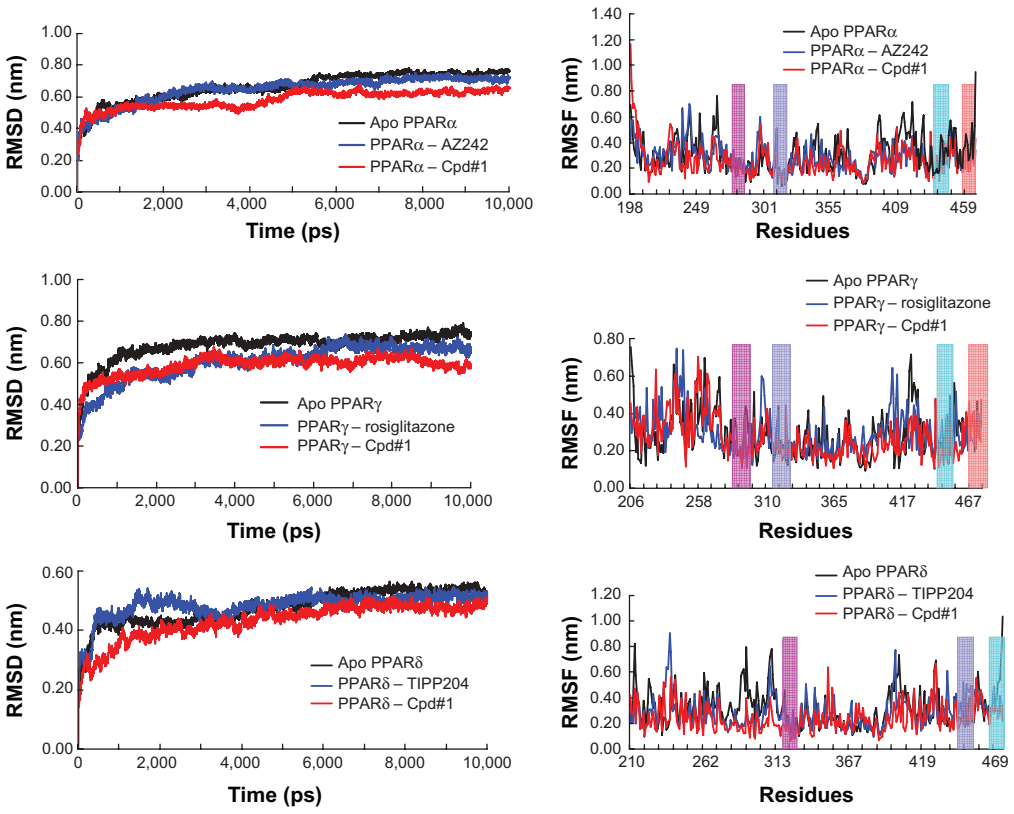

Figure 4 The molecular dynamics simulation results of PPARs–Cpd#1 complex.
Notes: The black line indicates the outcome for the system of the receptor alone without any ligand; the blue line indicates the outcome for the system of the receptor with the orignal ligand; and the red line indicates the outcome for the system of the receptor with the ligand Comp#1.
Abbreviations: PPAR, peroxisome proliferator-activated receptor; RMSD, root mean square deviation; RMSF, root mean square fluctuations.

Conclusion

In this study, rosiglitazone was modified by core hopping strategy to produce various analogues. Using docking and ADMET prediction technique, eight novel compounds were identified as multitargeted PPARα/γ/δ pan agonists with excellent pharmacokinetic properties. Molecular dynamics simulations of the representative Cpd#1 showed that Cpd#1 bound steadily to PPARα/γ/δ active site and restricted the target movement. These compounds have not been reported in the literature and could act as novel PPARs multitargeted agonists for antidiabetic drug research.

Acknowledgments

This work was supported by the National Natural Science Foundation of China (21202120), a China Postdoctoral Science Foundation funded project (2012T50237). The authors wish to thank the anonymous reviewers for their valuable suggestions, which were very helpful for strengthening the presentation of this study.

Disclosure

The authors report no conflicts of interest in this work.

References

1. Monsalve FA, Pyarasani RD, Delgado-Lopez F, Moore-Carrasco R. Peroxisome proliferator-activated receptor targets for the treatment of metabolic diseases. *Mediators Inflamm.* 2013;2013:549627.
2. Aleshin S, Strokin M, Sergeeva M, Reiser G. Peroxisome proliferator-activated receptor (PPAR) beta/delta, a possible nexus of PPARalpha- and PPARgamma-dependent molecular pathways in neurodegenerative diseases: review and novel hypotheses. *Neurochem Int.* 2013;63(4):322–330.
3. Seok H, Cha BS. Refocusing peroxisome proliferator activated receptor-alpha: a new insight for therapeutic roles in diabetes. *Diabetes Metab.* 2013;37(5):326–332.
4. Markt P, Petersen RK, Flindt EN, et al. Discovery of novel PPAR ligands by a virtual screening approach based on pharmacophore modeling, 3D shape, and electrostatic similarity screening. *J Med Chem.* 2008;51(20):6303–6317.
5. Antonelli A, Ferrari SM, Fallahi P, et al. Monokine induced by interferon gamma (IFNgamma) (CXCL9) and IFNgamma inducible T-cell alpha-chemoattractant (CXCL11) involvement in Graves' disease and ophthalmopathy: modulation by peroxisome proliferator-activated receptor-gamma agonists. *J Clin Endocrinol Metab.* 2009;94(5):1803–1809.
6. Antonelli A, Fallahi P, Ferrari SM, et al. Dedifferentiated thyroid cancer: a therapeutic challenge. *Biomed Pharmacother.* 2008;62(8):559–563.
7. Eldor R, DeFronzo RA, Abdul-Ghani M. In vivo actions of peroxisome proliferator-activated receptors: glycemic control, insulin sensitivity, and insulin secretion. *Diabetes Care.* 2013;36 Suppl 2:162–174.
8. Kostapanos MS, Kei A, Elisaf MS. Current role of fenofibrate in the prevention and management of non-alcoholic fatty liver disease. *World J Gastroentero.* 2013;5(9):470–478.
9. Lewis SN, Brannan L, Guri AJ, et al. Dietary alpha-eleostearic acid ameliorates experimental inflammatory bowel disease in mice by activating peroxisome proliferator-activated receptor-gamma. *PLoS One.* 2011;6(8):e24031.
10. Nissen SE, Wolski K. Effect of rosiglitazone on the risk of myocardial infarction and death from cardiovascular causes. *N Engl J Med.* 2007;356(24):2457–2471.
11. Wickens P, Zhang C, Ma X, et al. Indanylacetic acids as PPAR-delta activator insulin sensitizers. *Bioorg Med Chem Lett.* 2007;17(15):4369–4373.
12. Batista FA, Trivella DB, Bernardes A, et al. Structural insights into human peroxisome proliferator activated receptor delta (PPAR-delta) selective ligand binding. *PloS One.* 2012;7(5):e33643.
13. Rubenstrunk A, Hanf R, Hum DW, Fruchart JC, Staels B. Safety issues and prospects for future generations of PPAR modulators. *Biochim Biophys Acta.* 2007;1771(8):1065–1081.
14. Ma Y, Wang SQ, Xu WR, Wang RL, Chou KC. Design novel dual agonists for treating type-2 diabetes by targeting peroxisome proliferator-activated receptors with core hopping approach. *PloS One.* 2012;7(6):e38546.
15. Cronet P, Petersen JF, Folmer R, et al. Structure of the PPARalpha and -gamma ligand binding domain in complex with AZ242; ligand selectivity and agonist activation in the PPAR family. *Structure.* 2001;9(8):699–706.
16. Nolte RT, Wisely GB, Westin S, et al. Ligand binding and co-activator assembly of the peroxisome proliferator-activated receptor-gamma. *Nature.* 1998;395(6698):137–143.
17. Oyama T, Toyota K, Waku T, et al. Adaptability and selectivity of human peroxisome proliferator-activated receptor (PPAR) pan agonists revealed from crystal structures. *Acta Crystallogr D Biol Crystallogr.* 2009;65(Pt 8):786–795.
18. Banks JL, Beard HS, Cao Y, et al. Integrated modeling program, applied chemical theory (IMPACT). *J Comput Chem.* 2005;26(16):1752–1780.
19. Zapata-Sudo G, Lima LM, Pereira SL, et al. Docking, synthesis and anti-diabetic activity of novel sulfonylhydrazone derivatives designed as PPAR-gamma agonists. *Curr Top Med Chem.* 2012;12(19):2037–2048.
20. Cai L, Wang Y, Wang JF, Chou KC. Identification of proteins interacting with human SP110 during the process of viral infections. *Med Chem.* 2011;7(2):121–126.
21. Chou KC, Wei DQ, Zhong WZ. Binding mechanism of coronavirus main proteinase with ligands and its implication to drug design against SARS. *Biochem Bioph Res Co.* 2003;308(1):148–151.
22. Liao QH, Gao QZ, Wei J, Chou KC. Docking and molecular dynamics study on the inhibitory activity of novel inhibitors on epidermal growth factor receptor (EGFR). *Med Chem.* 2011;7(1):24–31.
23. Irwin JJ, Shoichet BK. ZINC – a free database of commercially available compounds for virtual screening. *J Chem Inf Model.* 2005;45(1):177–182.
24. da Silva FM, dos Santos JC, Campos JL, et al. Structure-based identification of novel PPAR gamma ligands. *Bioorg Med Chem Lett.* 2013;23(21):5795–5802.
25. Nevin DK, Peters MB, Carta G, Fayne D, Lloyd DG. Integrated virtual screening for the identification of novel and selective peroxisome proliferator-activated receptor (PPAR) scaffolds. *J Med Chem.* 2012;55(11):4978–4989.
26. Guasch L, Sala E, Mulero M, et al. Identification of PPARgamma partial agonists of natural origin (II): in silico prediction in natural extracts with known antidiabetic activity. *PloS One.* 2013;8(2):e55889.
27. Guasch L, Sala E, Castell-Auvi A, et al. Identification of PPARgamma partial agonists of natural origin (I): development of a virtual screening procedure and in vitro validation. *PloS One.* 2012;7(11):e50816.
28. Fruchart JC. Selective peroxisome proliferator-activated receptor alpha modulators (SPPARMalpha): the next generation of peroxisome proliferator-activated receptor alpha agonists. *Cardiovasc Diabetol.* 2013;12:82.
29. Liu L, Ma Y, Wang RL, Xu WR, Wang SQ, Chou KC. Find novel dual-agonist drugs for treating type 2 diabetes by means of cheminformatics. *Drug Des Dev Ther.* 2013;7:279–288.

30. Schuttelkopf AW, van Aalten DM. PRODRG: a tool for high-throughput crystallography of protein-ligand complexes. *Acta Crystallogr D Biol Crystallogr.* 2004;60(Pt 8):1355–1363.
31. Bernardes A, Souza PC, Muniz JR, et al. Molecular mechanism of peroxisome proliferator-activated receptor alpha activation by WY14643: a new mode of ligand recognition and receptor stabilization. *J Mol Biol.* 2013;425(16):2878–2893.
32. Puhl AC, Bernardes A, Silveira RL, et al. Mode of peroxisome proliferator-activated receptor gamma activation by luteolin. *Mol Pharmacol.* 2012;81(6):788–799.
33. Kouskoumvekaki I, Petersen RK, Fratev F, et al. Discovery of a novel selective PPARgamma ligand with partial agonist binding properties by integrated in silico/in vitro work flow. *J Chem Inf Model.* 2013;53(4):923–937.
34. Lian P, Wei DQ, Wang JF, Chou KC. An allosteric mechanism inferred from molecular dynamics simulations on phospholamban pentamer in lipid membranes. *PloS One.* 2011;6(4):e18587.
35. Wang YJ, Wang JF, Ping J, et al. Computational studies on the substrate interactions of influenza A virus PB2 subunit. *PloS One.* 2012;7(9):e44079.
36. Li XB, Wang SQ, Xu WR, Wang RL, Chou KC. Novel inhibitor design for hemagglutinin against H1N1 influenza virus by core hopping method. *PloS One.* 2011;6(11):e28111.
37. Issemann I, Prince RA, Tugwood JD, Green S. The peroxisome proliferator-activated receptor: retinoid X receptor heterodimer is activated by fatty acids and fibrate hypolipidaemic drugs. *J Mol Endocrinol.* 1993;11(1):37–47.
38. Feng G, Evangelisti L, Favero LB, Grabow JU, Xia Z, Caminati W. On the weak O-H···halogen hydrogen bond: a rotational study of CH3CHClF···H2O. *Phys Chem Chem Phys*. 2011;13(31):14092–14096.
39. Taylor R. Life-science applications of the cambridge structural database. *Acta Crystallogr D Biol Crystallogr.* 2002;58(Pt 6 No 1):879–888.
40. Eghdamian B, Ghose K. Mode of action and adverse effects of lipid lowering drugs. *Drug Today.* 1998;34(11):943–956.
41. Lipinski CA. Chris lipinski discusses life and chemistry after the rule of five. *Drug Discov Today.* 2003;8(1):12–16.
42. Egan WJ, Lauri G. Prediction of intestinal permeability. *Adv Drug Deliv Rev.* 2002;54(3):273–289.